Eur Biophys J (2006) 35:601–609
DOI 10.1007/s00249-006-0066-6

ARTICLE

A quasi-Laue neutron crystallographic study of D-xylose isomerase

Flora Meilleur · Edward H. Snell · Mark J. van der Woerd · Russell A. Judge · Dean A. A. Myles

Received: 15 February 2006 / Revised: 29 March 2006 / Accepted: 4 April 2006 / Published online: 4 May 2006

Abstract The location of hydrogen atoms in enzyme structures can bring critical understanding of catalytic mechanism. However, whilst it is often difficult to determine the position of hydrogen atoms using X-ray crystallography even with subatomic (< 1.0 Å) resolution data available, neutron crystallography provides an experimental tool to directly localize hydrogen/deuterium atoms in biological macromolecules at resolution of 1.5–2.0 Å. D-Xylose isomerase (D-xylose ketol-isomerase, EC 5.3.1.5) is a 43 kDa enzyme that catalyses the first reaction in the catabolism of D-xylose. Linearization and isomerization of D-xylose at the active site of D-xylose isomerase rely upon a complex hydrogen transfer. Neutron quasi-Laue data at 2.2 Å resolution were collected at room temperature on a partially deuterated *Streptomyces rubiginosus* D-xylose isomerase crystal using the LADI instrument at ILL with the objective to provide insight into the enzymatic mechanism. The neutron structure shows unambiguously that residue His 53 is doubly protonated at the active site of the enzyme. This suggests that the reaction proceeds through an acid catalyzed opening of the sugar ring, which is in accord with the mechanism suggested by Fenn et al. (Biochemistry 43(21): 6464–6474, 2004). This is the first report of direct observation of double protonation of His 53 and the first validation of the ring opening mechanism at the active site of D-xylose isomerase.

F. Meilleur (✉)
Institut Laue Langevin, BP 156, 38042 Grenoble, France
e-mail: meilleur@ill.fr

E. H. Snell
Hauptman-Woodward Medical Research Institute,
700 Ellicott Street, Buffalo, NY 14203, USA

M. J. van der Woerd
BAE Systems, 308 Voyager Way, Huntsville,
AL 35806, USA

R. A. Judge
Abbott Laboratories, Abbott Park, IL 60064, USA

D. A. A. Myles
Oak Ridge National Laboratory, P.O. Box 2008,
Oak Ridge, TN 37831, USA

Introduction

D-Xylose isomerase (D-xylose ketol-isomerase, EC 5.3.1.5) naturally catalyses the first reaction in the catabolism of D-xylose, but is also able to convert D-glucose to D-fructose. The conversion of D-xylose to D-xylulose or of D-glucose to D-fructose requires the transfer of a hydrogen atom between carbon C1 and C2 of the substrate. The mechanistic interest in D-xylose isomerase originates from the fact that the enzyme appears to catalyze an isomerization reaction not by proton-transfer mechanism but by a hydride shift promoted by a bridged bimetallic center. The metal ion normally found in the active site in D-xylose isomerase is magnesium.

Experimental evidence supports a 2-step mechanism in which substrates first bind to the enzyme in their closed ring form. The initial step of the reaction is then an enzyme-catalyzed ring opening of the substrate (Whitlow et al. 1991). Several mechanisms have been proposed. Lavie et al. (1994) suggest that Lys 182, which makes a hydrogen bond with the O1 atom of the

linear sugar, or a metal bound hydroxide ion, could trigger the substrate ring opening step. Other X-ray diffraction studies suggest that the His 53 and Asp 56 residues are important in the ring opening step (Collyer et al. 1990; Whitlow et al. 1991). In a mechanism proposed by Asboth and Naray-Szabo (2000), His 53 accepts a proton from the O1 atom of the sugar hydroxyl and transfers it to the O5 position. The sugar ring opens only after the proton then starts moving from NE2 of His 53 towards O5 of the sugar. The approach of Asp 56 towards His 53, which enhances the basicity of the histidine side chain, is thought to initiate the ring opening in this model. However, a recent high resolution structure of glucose bound D-xylose isomerase suggests a different model, in which His 53, protonated at the NE2 position, catalyzes the ring opening step through donation of a proton to the sugar O5 position (Fenn et al. 2004). The precise protonation state of His 53 is then of critical interest, but hydrogen atoms could not be directly observed at the 0.95 Å resolution of this structure.

The binding of the linearized substrate requires the subsequent formation of two bonds with the structural metal site (or metal 1) through O2 and O4 and also by coordinating through O2 and O1 to the catalytic metal (or metal 2).

In the isomerization reaction itself, a base-catalyzed proton transfer mechanism has been proposed, based upon the similarity of the xylose isomerase reaction and the reaction catalyzed by triosephosphatase isomerase(Allen et al. 1994a, b). However, X-ray crystallographic analyses showed no properly positioned base at the active site. Moreover, isotopic exchange kinetic studies do not support a proton transfer (Allen et al. 1994a, b). An alternative mechanism was proposed suggesting an isomerisation by 1,2-hydride shift (Collyer et al. 1990; Whitlow et al. 1991). Details of such a metal mediated hydride shift were described by Lavie et al. (1994).

The active site is formed by residues Asp 56, 216, 244, 254, 256 and 286, His 53 and 219, Glu 180 and two metal ion cofactors (Mg^{2+} or Mn^{2+}). In crystal structures of the substrate free enzyme, metal site 1 has been reported in two coordination states. Whilst Jenkins et al. (1992) and Lavie et al. (1994) report a tetra coordination of the ion with Glu 180, Glu 216, Asp 244 and Asp 286, Whitlow et al. (1991) and Carrel et al. (1989) described an octahedral coordination in which two water ligands were observed in addition to the four protein ligands. The discrepancy may arise from the difference in metal ions; magnesium (Jenkins et al. 1992; Lavie et al. 1994) versus manganese (Whitlow et al. 1991). At metal site 2, the catalytic ion is octahedrally coordinated in all published structures, with ligands Glu 216, His 219, Glu 254 (bidental coordination) and one water molecule. Lavie et al. (1994) note that the refined distance between the catalytic metal ion and its water ligand (1.9 Å) would be more consistent with a hydroxide ligand.

The available X-ray and biochemical data do not allow a full understanding of the enzymatic mechanism of xylose isomerase. In particular, the role of the catalytic metal ion remains unclear and the protonation state of catalytic residues remain unknown. Neutron crystallography can reveal hydrogen/deuterium atom positions in protein structures at resolution of 1.5–2.0 Å (Bon et al. 1999; Shu et al. 2000; Coates et al. 2001; Blakeley et al. 2004; Kurihara et al. 2004), because the neutron scattering factors for hydrogen and deuterium are closely similar to those of carbon, nitrogen and oxygen (see Table 1 and Meilleur et al. 2006). We have therefore performed a neutron structure analysis of D-xylose isomerase in order to clarify details of critical residues at the active site of D-xylose isomerase. Neutron quasi-Laue data were collected on *Streptomyces rubiginosus* D-xylose isomerase crystal at 2.2 Å resolution using the LADI instrument at ILL (Myles et al. 1998). The neutron structure unambiguously reveals the protonation state of His 53.

Materials and methods

Crystallization

D-Xylose isomerase was supplied by Genencor International. It was further purified using size exclusion chromatography on a BioRad Biologic chromatography system with Sephacryl S-200 high-resolution media and a 0.05 M sodium phosphate pH 7.7, 0.1 M sodium chloride, 0.02% azide running buffer. The main peak was collected and the fractions from numerous runs were pooled and dialyzed against distilled water at room temperature with a final dialysis against 0.05 g/L magnesium sulfate. Analyses showed the enzyme to be 96% pure.

Table 1 Coherent scattering lengths and incoherent scattering cross-sections for atoms in biological macromolecules

	H	D	C	N	O
Bcoh (fm)	–3.74	+6.67	+6.65	+9.36	+5.81
σcoh (barns)	1.76	5.59	5.56	11.03	4.23
σinc (barns)	80.27	2.05	0	0.49	0

In order to reduce the high background of the neutron diffraction experiment that arises from the large incoherent cross section of hydrogen, D-xylose isomerase crystals were grown in deuterated solvents. The purified D-xylose isomerase solution was repeatedly diluted with deuterated 0.05 g/L magnesium sulfate solution and concentrated by centrifugal ultra filtration. Deuterated ammonium sulfate solution was made by dissolving ammonium sulfate salt in deuterium oxide (D_2O) and adjusted to pH 7.7. Large crystals were grown in 1.5 ml Eppendorf tubes using the batch method with 15% ammonium sulfate, 72 mg/ml D-xylose isomerase at pH 7.7 and a temperature of 22°C, conditions which were adapted from our previous results (Snell et al. 2006).

Neutron data collection and reduction

Crystal samples were transported in the Eppendorf tubes they were grown in from the NASA Marshall Space Flight Center, Alabama, USA, to the Institut Laue Langevin in Grenoble, France. A crystal of about $1 \times 2 \times 2$ mm^3 was mounted in a 5 mm diameter quartz capillary. Crystal hydration was maintained with reservoirs of crystallization solution placed on both capillary ends. Wax was used for sealing. Neutron quasi-Laue data were collected at 293 K on the LADI beamline installed on the end-station T17 of cold neutron guide H142 at ILL (Cipriani et al. 1996; Myles et al. 1998). A Ni/Ti multilayer wavelength selector was used to select a narrow wavelength band pass ($\Delta\lambda/\lambda \sim 25\%$). Each image covers approximately 8 degrees of reciprocal space. Data were collected from two crystal orientations to help fill the blind region and therefore increase completeness. The crystal belongs to space group I222. The unit cell parameters were refined to $a = 92.79$ Å, $b = 98.37$ Å and $c = 101.51$ Å. In order to limit the number of spatially overlapped reflections arising from the large unit cell parameters, the wavelength range was tuned towards longer wavelengths compared to previous experiments and the crystal illuminated with a 3.10–4.50 Å wavelength range centered at 3.8 Å. A total of 21 images of 24 h exposure each were collected. A typical diffraction pattern is shown in Fig. 1.

The neutron Laue data were processed using the Daresbury Laboratory software *LAUEGEN* modified to account for the cylindrical geometry of the detector (Campbell et al. 1998). The program *LSCALE* (Arzt et al. 1999) was used to derive the wavelength-normalization curve using the intensity of symmetry equivalent reflections measured at different wavelengths. The internal agreement factor from *LSCALE* for the intensities of reflections with wavelength differences of less than 0.1 Å was 13.9%. The data were then scaled and merged using *AGROVATA* and *ROTAVATA* (Collaborative Computational Project, Number 4, 1994). Data reduction statistics are summarized in Table 2. The overall *R*-factor is 11.3% (16.4% in the highest shell of resolution) and the overall $I/\sigma(I)$ is 5.1 (4.3 in the highest shell of resolution).

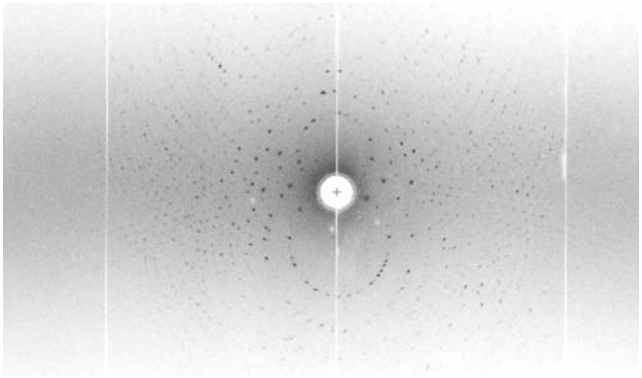

Fig. 1 Typical quasi-Laue diffraction pattern from xylose isomerase

Neutron structure refinement

The neutron structure was refined using *CNSsolve* (Brunger et al. 1998) starting from a high resolution X-32ray structure of D-xylose isomerase, omitting all water molecules. The protein structure was composed of 3,064 ''heavy'' atoms (C, N, O, S) and 2,880 hydrogen/deuterium atoms, hence a total of 5,944 atoms. The position of non-hydrogen/deuterium atoms were held at their X-ray refined positions since the number of refinable parameters (position and isotropic *B*-factor of each atom, i.e., $4 \times 5{,}944 = 23{,}776$ parameters) was large compared to the number of unique reflections available from the neutron data set (14,491). The need to refine exchangeable hydrogen/deuterium (H/D) occupancy added further complication. Hydrogen and deuterium positions were generated from the starting X-ray model using the topology and parameter files ''protein-allhdg.top'' and ''protein-allhdg.param'', from the *CNS* package specific to NMR refinement (Brunger et al. 1998). Initially all exchangeable hydrogen positions, i.e., those bound to oxygen or nitrogen, were replaced by deuterium. Appropriate neutron-scattering lengths were used throughout all subsequent refinement steps (International Tables for Crystallography, 1995, vol. *C*, pp 384–391). In all refinement procedures 3.5% of the data were omitted for R_{free} calculation.

Rigid body refinement against all neutron data to 2.2 Å reduced the working *R*-factor from 35.5 to 34.9%

Table 2 Neutron diffraction data statistics

d_{min} (Å)	Completness (%)	Multiplicity	R^{a}_{merge}	R^{b}_{cum}	I/sigma(I)
6.58	91.4	3.3	0.093	0.093	6.3
5.25	94.1	3.5	0.100	0.096	6.3
4.50	91.3	3.4	0.105	0.099	5.5
4.00	90.1	3.0	0.107	0.101	5.4
3.64	85.2	2.7	0.111	0.103	5.5
3.36	80.8	2.5	0.113	0.104	5.5
3.13	73.0	2.4	0.116	0.105	5.7
2.95	66.3	2.2	0.125	0.106	5.4
2.80	57.8	2.1	0.131	0.107	5.4
2.66	54.0	2.1	0.137	0.108	4.9
2.55	50.3	2.1	0.141	0.109	4.9
2.44	46.2	2.1	0.149	0.110	4.5
2.35	46.6	2.1	0.151	0.111	4.6
2.27	44.5	2.0	0.154	0.112	4.6
2.20	42.7	2.0	0.164	0.113	4.3
Total	61.4	2.5		0.113	5.1

a $R_{merge} = \sum_{hkl}\sum_{i}\left|I_i(hkl) - \overline{I(hkl)}\right| \Big/ \sum_{hkl}\sum_{i} I_i(hkl)$

b R_{cum} R_{merge} up to this range

(R_{free} 34.8%). Examination of the neutron density maps ($2F_o$–F_c and F_o–F_c) using the program O (Jones et al. 1991) identified 124 water sites. Deuterium atoms were generated for these water molecules using modified water topology and parameter files. Waters were manually fitted in the neutron density using the program O (Jones et al. 1991). Water molecules were included and refined from the early stages of the refinement because the contribution of ordered deuterated solvent to the neutron scattering density is large. Following B-factor refinement of all protein and water atoms, the working R-factor improved to 32.5% (R_{free} = 32.9%). The next steps consisted of the refinement of first the positions, then the B-factors and finally the H/D occupancies of the exchangeable hydrogen atom positions. Currently, the working R-factor and R_{free} are 30.8 and 32.1%, respectively. The R-values are higher than for a comparable X-ray structure, which is typical of other larger neutron protein structures (Niimura et al. 1997; Bon et al. 1999; Habash et al. 2000; Coates et al. 2001), but given the number of observations (14,491) and refinable parameters (23,776), do suggest that the current model adequately explains the available data.

Results

Extent of backbone deuteration

The extent of the backbone deuterium substitution was assessed by performing an occupancy refinement of the amide backbone H/D exchange following the refinement protocol described by Wlodawer et al. (1989). In this approach, exchangeable amide hydrogen sites are assigned the neutron scattering length of deuterium. Occupancies that refined to –0.56 give strong indication that deuterium exchange did not occur ($-0.56 \times b_D = b_H$), whereas occupancies that refined to + 1.00 suggested that full exchange occurred (Fig. 2). Following Wlodawer's criterion, 177 backbone amide sites (48%) were assigned as fully occupied D sites (D occupancy > 0.75), while 67 (18%) were assigned as fully occupied H sites (H occupancy > 0.75) (Table 3). At the remaining 34% of the backbone amide sites, exchange was considered incomplete. Figure 3 shows the distribution of the H/D exchanged sites over the protein. The regions protected from exchange appeared to be mostly the buried β-strand core as well as two α-helices. Deuterium occupancy refinement improved slightly the R factors (R_{work} = 31.5% (from 32.5%) and R_{free} = 32.5% (from 32.7%)).

Side chains

Whilst most exchangeable deuterium atoms were clearly visible on side chains, hydrogen atoms were poorly visible at the resolution (2.2 Å) of this analysis. This may be due to the weak and negative neutron scattering factor of hydrogen (–0.3739E-12 cm), which can lead to cancellation when overlapped with the positive scattering densities of neighboring carbon, oxygen, and nitrogen atoms at this resolution (Shu et al. 2000). Figure 4a shows neutron density for Trp 136 and Fig. 4b shows that for Lys 182, where the N-D3 group is clearly visible.

The conformations of asparagine and glutamine side chains are not always clear from X-ray analysis, because it is difficult to distinguish between oxygen and nitrogen atoms, and conformation is normally assigned

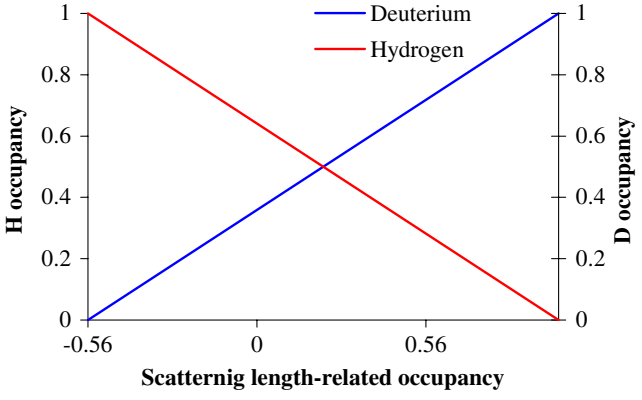

Fig. 2 Hydrogen/deuterium occupancy factors

Table 3 Distribution of deuterium and hydrogen as a function of occupancy

Hydrogen occupancy	Number of hydrogen atom	Deuterium occupancy	Number of deuterium atom
1.00	34	1.00	97
[0.96; 1.00]	4	[0.94; 1.00]	20
[0.90; 0.96]	10	[0.87; 0.94]	20
[0.83; 0.90]	10	[0.81; 0.87]	18
[0.77; 0.83]	9	[0.74; 0.81]	22

indirectly based upon likely hydrogen bonding interactions. In contrast, the neutron density for these residues is markedly asymmetric, due to the presence of two deuterium atoms bound to the nitrogen, and the orientation of the side chains is normally unambiguous. Figure 5a shows neutron density for the well-ordered Gln 248 side chain, which makes three hydrogen bonds with neighboring backbone atoms. Figure 5b shows neutron density for Gln 376, which reveals the correct side chain orientation of this residue. Similarly, the orientation of OD groups in tyrosine, serine and threonine residues could be reliably determined by neutron map inspection (Fig. 6).

The protonation states of aspartic and glutamic residues were examined. There are 29 aspartate residues, one of which is at the active site (Asp 180), and 35 glutamic residues, five of which are at the active site (Glu 56, 244, 254, 256, and 286). Four aspartic residues present neutron density features that indicate protonation, such as Asp 140 depicted in Fig. 6a. The protonation states of all 10 histidine residues was evaluated, first by close inspection of the neutron maps and then by refining the H/D occupancies of DD1 (bound to ND1) and DE2 (bound to NE2) atoms according to the protocol of Wlodawer et al. (1989). The results clearly indicate that six His residues (His 53, 70, 95, 229, 284, 381) are doubly protonated, and that four residues are singly protonated; His 48 and His 197 at position NE2, and His 219 and His 242 at position ND1 (Meilleur 2004).

Water molecules

A total of 124 water (D_2O) molecules were modeled by inspection of F_o–F_c and $2F_o$–F_c neutron density maps. The molecules were manually oriented in the neutron density, taking into account the geometry of possible hydrogen bonds between them and the surrounding protein residues or neighbor water molecules. All 124 water molecules were found in close proximity to X-ray refined water oxygen atom positions. Figure 7 shows an example of a D_2O water molecule positioned and oriented in the $2F_o$–F_c neutron density map.

Protonation state at the active site

The critical residues of the active site are one aspartic residue, Asp 180, five glutamic residues, Glu 56, 244, 254, 256, 286, two histidine residues His 53 and 219, two metal ions and their coordination water molecules. Careful inspection of the neutron structure suggests that none of the active site carboxylic acid groups are protonated. However, the maps clearly show that His 219 is singly protonated at nitrogen atom ND1, which is in accord with the fact that it is ligated to the catalytic metal ion (Fig. 8). Crucially, the neutron density at the second active site histidine, His 53, clearly shows that this residue is doubly protonated at both ND1 and NE2 positions (Fig. 9). This is of particular interest, since His 53 is thought to be involved in the opening of the substrate ring, and the protonation state of this residue has been a matter of some conjecture.

Superposition and comparison of the neutron and X-ray models at metal site 2 show that the magnesium ion cannot be visualized in the neutron maps at the

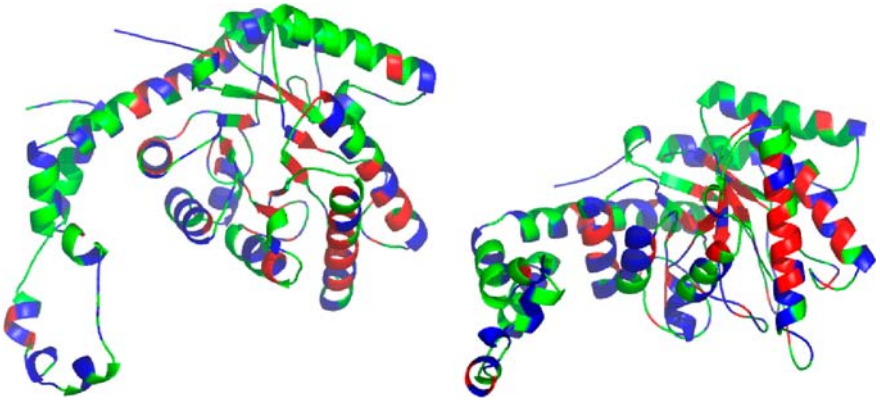

Fig. 3 Extent of backbone deuteration of xylose isomerase in two orthogonal views. *Green* deuterium occupancy > 0.75 suggesting full exchange; *red* hydrogen occupancy > 0.75 suggesting no exchange; *blue* intermediate occupancy value suggesting partial exchange

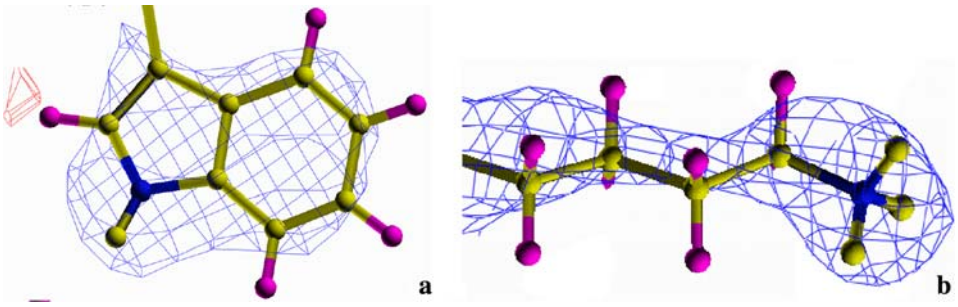

Fig. 4 **a** Tryptophan 136. *Blue* $2F_o$–F_c neutron map contoured at 1σ level. *Red* $2F_o$–F_c neutron map contoured at –3σ level. **b** Lysine 182 shows positive density for the ND_3^+ group. *Blue* $2F_o$–F_c neutron map contoured at 1σ level

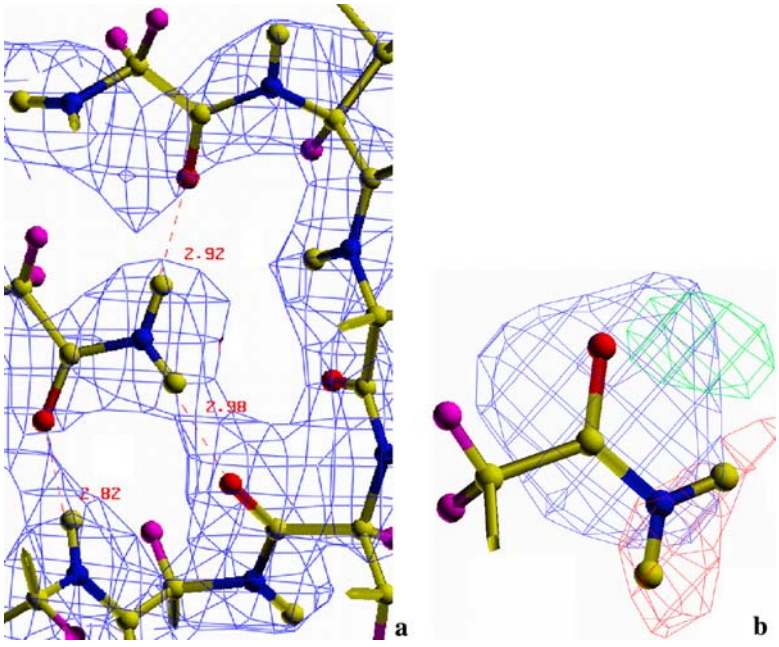

Fig. 5 Glutamine 248 side chain. **a** Hydrogen bonds made by Gln 248. **b** F_o–F_c neutron density suggesting an alternate conformation of Gln 376. *Blue* $2F_o$–F_c neutron map contoured at 1.5σ level. *Green* F_o–F_c neutron map contoured at 2.5σ level. *Red* F_o–F_c neutron map contoured at –2.5σ level

position determined for the metal ion in the X-ray structure (marked in Fig. 10). Metal ions scatter neutrons much more weakly than X-rays, and this result may reflect the low neutron scattering factor of a single magnesium ion (0.5375E-12 cm), which is less than that of a single deuterium atom. There is, however, significant density in the neutron map at a position that corresponds to the position of a solvent ligand to the

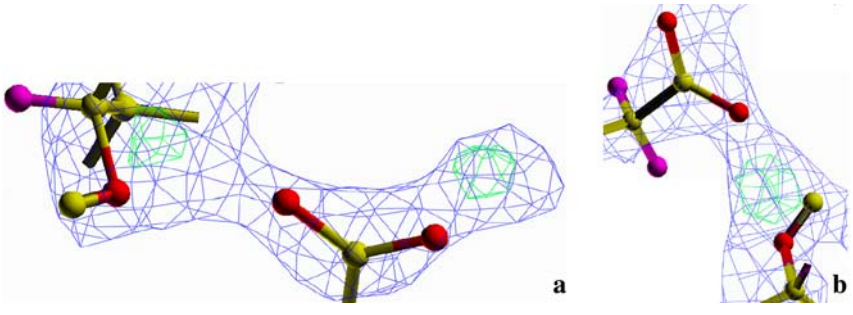

Fig. 6 Conformation of side chain threonine OD groups. **a** Thr 104–Glu 140. The F_o–F_c positive neutron density features suggest a misorientation of the Thr 104 OD group and the protonation of Glu 140. **b** Thr 292–Asp 291. The F_o–F_c positive neutron density feature suggests a misorientation of the threonine OD group. The deuterium position suggested by the F_o–F_c neutron map is more favorable to the formation of a hydrogen bond between the two side chains. *Blue* $2F_o$–F_c neutron map contoured at 1σ and 1.5σ level, for **a** and **b**, respectively. *Green* F_o–F_c neutron map contoured at 3σ level

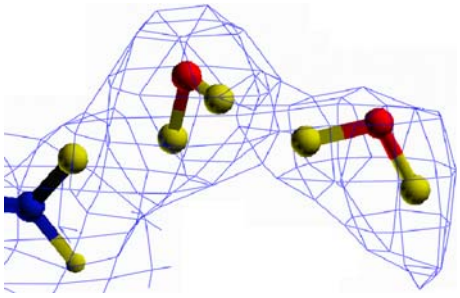

Fig. 7 D_2O water molecules. *Blue* $2F_o–F_c$ neutron map contoured at 1.5σ level

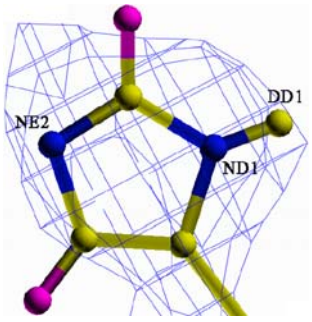

Fig. 8 Histidine 219. *Blue* $2F_o–F_c$ neutron map contoured at 1.5σ

metal ion as observed in the X-ray structure (Fig. 10). The visibility of D_2O water molecules are normally enhanced in neutron maps because the neutron scattering lengths of deuterium and oxygen are similar (total scattering = 0.5803E-12 (O) + 2 × 0.6671E-12 (D_2) = 1.9145E-12 cm) (for example, see Fig. 7). However, when contoured at 1.4σ, the $2F_o–F_c$ neutron density at this position appears truncated, which could indicate a hydroxide ion OD^- (total scattering = 0.5803E-12 (O) + 0.6671E-12 (D) = 1.2474E-12 cm). Earlier X-ray studies of the substrate free enzyme suggested a hydride ion at this position (Lavie et al. 1994).

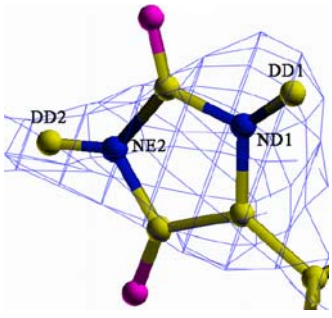

Fig. 9 Histidine 53. *Blue* $2F_o–F_c$ neutron map contoured at 1.5σ

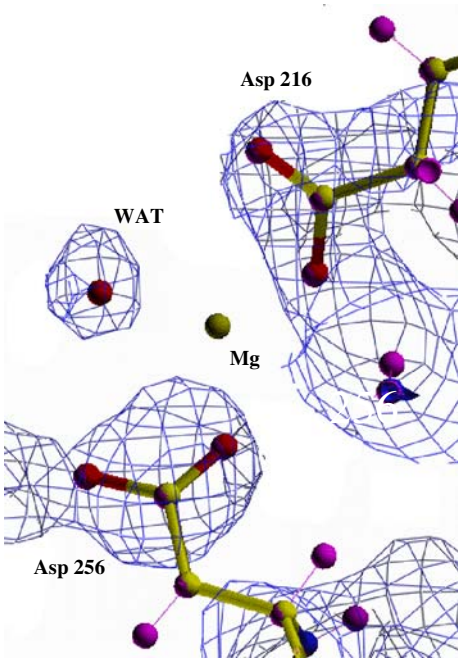

Fig. 10 X-ray model (*standard color*) at the Metal 2 site superimposed with the neutron model (*pink*). Mg and WAT positions are from the X-ray model. *Blue* $2F_o–F_c$ neutron map contoured at 1.4σ level

Discussion and conclusions

Good quality neutron data have been collected to 2.2 Å resolution from a large D-xylose isomerase crystal on the Laue diffractometer at ILL. D-Xylose isomerase is one of the largest systems ever studied at near atomic resolution by neutron crystallography, both in terms of molecular weight and unit cell parameters. Whilst deuterium atoms were clearly visible in the resulting maps, hydrogen atoms were more difficult to locate, most probably due to cancellation effects between the negative scattering density of hydrogen and positive density of neighboring carbon, nitrogen, and oxygen atoms at the 2.2 Å resolution of this neutron analysis (Shu et al. 2000).

The clear visibility of deuterium atoms in the neutron structure allowed the distribution and extent of H/D exchange at backbone amide positions to be mapped. This analysis shows that approximately 50% of the backbone amide hydrogen atoms could be confidently assigned as having completely exchanged for deuterium. The enhanced visibility of water molecules in neutron structures allowed a total of 124 water positions to be assigned, positioned and orientated as full D_2O molecules. At metal site 2 in the active site, truncated neutron density may indicate that a hydroxide ion (OD^-), rather than a water molecule (D_2O), is coordinated to the catalytic metal ion. This was previously proposed by

Lavie et al. (1994), based upon the distance between the solvent ligand oxygen atom and the metal ion observed in their X-ray structure. Higher resolution neutron data are required in order to confirm this.

Most importantly, the visibility of deuterium atoms in the structure allowed the protonation states of amino acid side chains at the active site of the enzyme to be determined. This is an important result. His 53 is thought to be involved in the first ring opening step of the acid-catalyzed mechanism, based upon analysis of steric constraints and geometry of the interactions at the active site (Fenn et al. 2004). However, hydrogen atom positions could not be seen in the atomic resolution X-ray structures of either the native, substrate bound or inhibitor bound D-xylose isomerase (PDB code 1MUW, 1S5M and 1S5N, respectively). Moreover, the protonation state of this residue cannot be reliably inferred from analysis of ND1–CE1 and CE1–NE2 bond lengths, because the observed differences in refined bond length are within the experimental error. With neutron diffraction we show unambiguously that His 53 is protonated/deuterated at both the ND1 and NE2 positions. This provides compelling evidence in support of the mechanism proposed by Fenn et al. (2004), which suggests that His 53 donates its HE2 proton to the sugar oxygen O5 to promote the ring opening. The neutron structure determination has thus helped clarify key details of this critical step in the acid-catalyzed mechanism of D-xylose isomerase.

This work demonstrates that neutron protein crystallography can provide a powerful adjunct to high resolution X-ray analysis when the location of hydrogen atoms in proteins is important to define biological function. This is likely to be of particular interest in understanding enzyme catalytic mechanisms, since X-ray crystallography alone is often unable to discriminate between chemically possible mechanisms. Whilst the technique is still technically demanding, developments worldwide to build optimized diffractometers at both new and existing neutron sources, and to ease the sample preparation will broaden the accessibility of the technique and open new possibilities.

Acknowledgments We would like to thank the Institut Laue Langevin for providing neutron beam time and Genencor International for the generous donation of the xylose isomerase. Richard Kephart is thanked for assistance in the initial stages of this project. EHS, MvdW and RAJ were supported through NASA grant NAG8-1916. EHS also acknowledges the Oishei Foundation for their generous financial support. DAAM acknowledges the support of the Laboratory Directed Research and Development Program of Oak Ridge National Laboratory, DOE Contract No. DE-AC05-00OR22725. The authors are especially grateful for the constructive referee input.

References

Arzt S, Campbell JW, Harding MM, Hao Q, Helliwell JR (1999) *LSCALE*—the new normalization, scaling and absorption correction program in the Daresbury *Laue* software suite. J Appl Cryst 32:554–562

Allen KN, Lavie A, Farber GK, Glasfeld A, Petsko GA, Ringe D (1994a) Isotopic exchange plus substrate and inhibition kinetics of D-xylose isomerase do not support a proton-transfer mechanism. Biochemistry 33(6):1481–1487

Allen KN, Lavie A, Glasfeld A, Tanada TN, Gerrity DP, Carlson SC, Farber GK, Petsko GA, Ringe D (1994b) Role of the divalent metal ion in sugar binding, ring opening, and isomerization by D-xylose isomerase: replacement of a catalytic metal by an amino acid. Biochemistry 33(6):1488–1494

Asboth B, Naray-Szabo G (2000) Mechanism of action of D-xylose isomerase. Curr Protein Pept Sci 1(3):237–254

Blakeley MP, Kalb AJ, Helliwell JR, Myles DA (2004) The 15-K neutron structure of saccharide-free concanavalin A. Proc Natl Acad Sci USA 101(47):16405–16410

Bon C, Lehmann MS, Wilkinson C (1999) Quasi-Laue neutron-diffraction study of the water arrangement in crystals of triclinic hen egg-white lysozyme. Acta Crystallogr D Biol Crystallogr 55(Pt 5):978–987

Brunger AT, Adams PD, Clore GM, DeLano WL, Gros P, Grosse-Kunstleve RW, Jiang JS, Kuszewski J, Nilges M, Pannu NS, Read RJ, Rice LM, Simonson T, Warren GL (1998) Crystallography & NMR system: a new software suite for macromolecular structure determination. Acta Crystallogr D Biol Crystallogr 54:905–921

Campbell JW, Hao Q, Harding MM, Nguti ND, Wilkinson C (1998) LAUEGEN version 6.0 and INTLDM. J Appl Cryst 31:496–502

Carrell HL, Glusker JP, Burger V, Manfre F, Tritsch D, Biellmann JF (1989) X-ray analysis of D-xylose isomerase at 1.9 A: native enzyme in complex with substrate and with a mechanism-designed inactivator. Proc Natl Acad Sci USA 86(12):4440–4444

Cipriani F, Castagna JC, Wilkinson C, Lehmann MS, Buldt G (1996) A neutron image plate quasi-Laue diffractometer for protein crystallography. Basic Life Sci 64:423–431

Coates L, Erskine PT, Wood SP, Myles DA, Cooper JB (2001) A neutron Laue diffraction study of endothiapepsin: implications for the aspartic proteinase mechanism. Biochemistry 40(44):13149–13157

Collyer CA, Henrick K, Blow DM (1990) Mechanism for aldose-ketose interconversion by D-xylose isomerase involving ring opening followed by a 1,2-hydride shift. J Mol Biol 212(1):211–235

Fenn TD, Ringe D, Petsko GA (2004) Xylose isomerase in substrate and inhibitor michaelis states: atomic resolution studies of a metal-mediated hydride shift. Biochemistry 43(21):6464–6474

Habash J, Raftery J, Nuttall R, Price HJ, Wilkinson C, Kalb AJ, Helliwell JR (2000) Direct determination of the positions of the deuterium atoms of the bound water in—concanavalin A by neutron Laue crystallography. Acta Crystallogr D Biol Crystallogr 56(Pt 5):541–550

Jenkins J, Janin J, Rey F, Chiadmi M, Van Tilbeurgh H, Lasters I, De Maeyer M, Van Belle D, Wodak SJ, Lauwereys M et al (1992) Protein engineering of xylose (glucose) isomerase from Actinoplanes missouriensis. 1. Crystallography and site-directed mutagenesis of metal binding sites. Biochemistry 31(24):5449–5458

Jones TA, Zou JY, Cowan SW, Kjeldgaard M (1991) Improved methods for building protein models in electron density maps and the location of errors in these models. Acta Crystallogr A 47(Pt2):110–119

Kurihara K, Tanaka I, Niimura N, Refai Muslih M, Ostermann A (2004) A new neutron single-crystal diffractometer dedicated for biological macromolecules (BIX-4). J Synchrotron Radiat 11:68–71

Lavie A, Allen KN, Petsko GA, Ringe D (1994) X-ray crystallographic structures of D-xylose isomerase-substrate complexes position the substrate and provide evidence for metal movement during catalysis. Biochemistry 33(18):5469–5480

Meilleur F (2004) Ph.D Thesis. University J. Fourier, Grenoble, France

Meilleur F, Myles DAA, Blakeley MP (2006) Neutron Laue macromolecular crystallography. Eur Biophys J (in press)

Myles DAA, Bon C, Langan P, Cipriani F, Castagna JC, Lehmann MS, Wilkinson C (1998) Neutron Laue diffraction in macromolecular crystallography. Physica B 241–243: 1122–30

Niimura N, Minezaki Y, Nonaka T, Castagna JC, Cipriani F, Hoghoj P, Lehmann MS, Wilkinson C (1997) Neutron Laue diffractometry with an imaging plate provides an effective data collection regime for neutron protein crystallography. Nat Struct Biol 4(11):909–914

Shu F, Ramakrishnan V, Schoenborn BP (2000) Enhanced visibility of hydrogen atoms by neutron crystallography on fully deuterated myoglobin. Proc Natl Acad Sci USA 97(8):3872–3877

Snell EH, van der Woerd MJ, Damon M, Judge RA, Myles DA, Meilleur F: Optimizing crystal volume for neutron diffraction (this issue)

Whitlow M, Howard AJ, Finzel BC, Poulos TL, Winborne E, Gilliland GL (1991) A metal-mediated hydride shift mechanism for xylose isomerase based on the 1.6 A *Streptomyces rubiginosus* structures with xylitol and D-xylose. Proteins 9(3):153–173

Wlodawer A, Savage H, Dodson G (1989) Structure of insulin: results of joint neutron and X-ray refinement. Acta Crystallogr B 45(Pt 1):99–107